

UNCLASSIFIED

Defense Technical Information Center  
Compilation Part Notice

ADP023706

TITLE: Visible Lesion Laser Thresholds in Cynomolgus [Macaca fascicularis] Retina with a 1064-nm, 12-ns Pulsed Laser

DISTRIBUTION: Approved for public release, distribution unlimited

This paper is part of the following report:

TITLE: Conference on Optical Interactions with Tissue and Cells [18th]  
Held in San Jose, California on January 22-24, 2007

To order the complete compilation report, use: ADA484275

The component part is provided here to allow users access to individually authored sections of proceedings, annals, symposia, etc. However, the component should be considered within the context of the overall compilation report and not as a stand-alone technical report.

The following component part numbers comprise the compilation report:

ADP023676 thru ADP023710

UNCLASSIFIED

# Visible Lesion Laser Thresholds in Cynomolgus (*Macaca fascicularis*) Retina with a 1064-nm, 12-ns Pulsed Laser

Jeffrey W. Oliver<sup>a</sup>, David J. Stolarski<sup>b</sup>, Gary D. Noojin<sup>b</sup>, Harvey M. Hodnett<sup>b</sup>, Michelle L. Imholte<sup>b</sup>,  
Benjamin A. Rockwell<sup>a</sup>, Semih S. Kumru<sup>a</sup>

<sup>a</sup>U.S. Air Force Research Laboratory (AFRL/HEDO), Brooks City-Base, TX 78235-5278;

<sup>b</sup>Northrop Grumman, 4241 Woodcock Dr., Suite B-100, San Antonio, TX 78228-1330

## ABSTRACT

A series of experiments in a new animal model for retinal damage, cynomolgus monkeys (*Macaca fascicularis*), have been conducted to determine the damage threshold for 12.5-nanosecond laser exposures at 1064 nm. These results provide a direct comparison to threshold values obtained in rhesus monkey (*Macaca mulatta*), which is the model historically used in establishing retinal maximum permissible exposure (MPE) limits. In this study, the irradiance level of a collimated Gaussian laser beam of 2.5 mm diameter at the cornea was randomly varied to produce a rectangular grid of exposures on the retina. Exposures sites were fundoscopically evaluated at post-irradiance intervals of 1 hour and 24 hours. Probit analysis was performed on dose-response data to obtain probability of response curves. The 50% probability of damage (ED<sub>50</sub>) values for 1 and 24 hours post-exposure are 28.5(22.7-38.4)  $\mu\text{J}$  and 17.0(12.9-21.8)  $\mu\text{J}$ , respectively. These values compare favorably to data obtained with the rhesus model, 28.7(22.3-39.3)  $\mu\text{J}$  and 19.1(13.6-24.4)  $\mu\text{J}$ , suggesting that the cynomolgus monkey may be a suitable replacement for rhesus monkey in photoacoustic minimum visible lesion threshold studies.

Keywords: Eyes; Minimum visible lesions; Retina; Cynomolgus monkey; Laser bioeffects; Pulsewidth; Nanosecond; Wavelength; Infrared lasers

## 1. INTRODUCTION

The non-human primate (NHP) model is accepted as the best animal model for human retinal eye injury. This model was adopted because it has excellent comparability in the thickness, absorption, reflection, pigmentation, and index of refraction of ocular components. The Indian-origin rhesus monkeys (*Macaca mulatta*) have been extensively utilized over the past 45 years in characterizing the light energy levels required to inflict retinal injury.

Driven primarily by reduced availability of rhesus monkeys, the need for a different animal model has arisen in our laboratory. The cynomolgus (*Macaca fascicularis*) has been suggested as the best replacement for the rhesus monkeys as a retinal eye injury model.

In migrating to this new model, the existing body of knowledge from the rhesus model needs to be experimentally tied to cynomolgus data. Therefore, this study was undertaken to tie (or “bridge”) rhesus data for retinal threshold levels (ED<sub>50</sub>) to comparable data obtained with the cynomolgus. It is not feasible to duplicate 45 years of rhesus experimentation to prove a worthy replacement model. The goal of the “Bridging” experiments is to provide a representative sample of cynomolgus data, using select parameters leading to damage by photothermal, photochemical, or photomechanical mechanisms, for comparison with rhesus experimental results.

There is substantial physiological justification for the selection of the cynomolgus monkey as a replacement for the rhesus including comparable retinal and choroidal pigmentation and vasculature, the presence of a fovea and similar

refractive properties. Comparative biometric data from cynomolgus monkey, rhesus monkey and human subjects is listed in Table 1. Furthermore, with suprathreshold retinal laser (argon ion laser, 514 nm) exposures, Wallow *et al.* has reported the morphological level of damage (RPE) and size of lesions to be very similar between human and cynomolgus.

Table 1. Comparative ocular biometric data from cynomolgus monkey, rhesus monkey and human subjects.

Ocular Structure	Cynomolgus [1, 2]	Rhesus [3, 4]	Human [5-7]
Corneal Thickness	$0.42 \pm 0.01$ mm	$0.47 \pm 0.02$ mm	0.52 mm*
Corneal Curvature	$6.4 \pm 0.2$ mm**	$6.39 \pm 0.06$ mm	$7.8 \pm 0.6$ mm
Anterior Chamber	$2.79 \pm 0.27$ mm	$3.48 \pm 0.09$ mm	3.54 mm*
Lens Thickness	$3.18 \pm 0.15$ mm	$3.62 \pm 0.05$ mm	3.81 mm*
Vitreous Cavity Length	$11.25 \pm 0.51$ mm	$12.44 \pm 0.17$ mm	$15.90 \pm 0.72$ mm
Axial Globe Length	$17.16 \pm 0.69$ mm	$19.45 \pm 0.20$ mm	$23.43 \pm 0.80$ mm
* Average of 10 emmetropic eyes Standard Deviation not Reported			
** Calculated from refractive power and index of refraction for cornea (1.376).			

The damage mechanism for retinal laser exposures in the 10-ns exposure regime is believed to be primarily photomechanical in nature. [8-11] Damage occurs as a result of the rapid deposition and conversion of laser energy at high peak irradiance levels (typically near the beam focus) into thermally-induced pressure gradients. These rapidly increasing pressure gradients result in the propagation of acoustic, or shock waves in the biological media. At short distances from their origin, the magnitude of these spherically expanding waves is sufficient to induce mechanical damage (shearing forces) to the membrane and structural proteins of cells. Several authors have presented results in the rhesus model with similar laser parameters as used in this study [12-14]. There is significant spread in the published data with the lowest threshold value reported from previous work completed by this laboratory (HEDO)[12]. The variance in data from previous studies in rhesus monkey is most likely a result of differences in experimental configuration including beam size at the cornea and laser beam quality.

Table 2. Prior MVL ED<sub>50</sub> data for retinal damage at 1064 nm using rhesus monkeys.

Reference	Pulse Duration	24 hour MVL ED50
[13]	15 ns	68 $\mu$ J
[14]	4 ns	158 $\mu$ J
[15]	20 ns	99 $\mu$ J
[12]	7 ns	19 $\mu$ J

This report, the first in a planned series of reports, compares retinal photomechanical damage induced in the cynomolgus monkey using single 12-ns, 1064-nm exposures, with historical data from rhesus monkey. The experimental configuration utilized in this study is substantially equivalent to that employed by Cain *et al.* with rhesus monkey. [12]

## 2. METHODS

### 2.1. Laser System

The laser system utilized in this set of experiments was a Nd:YAG, Q-switched laser (Spectra-Physics Model DCR-11) operating at 1064 nm. The beam divergence was less than 0.5 milliradians. The laser was verified to have an average pulse duration of 12.5 ns with a fast photodiode (Hamamatsu Model C1083) and a 500-MHz digital storage oscilloscope (Tektronix Model TDS30544B). A typical temporal profile for the laser is presented in Figure 1.

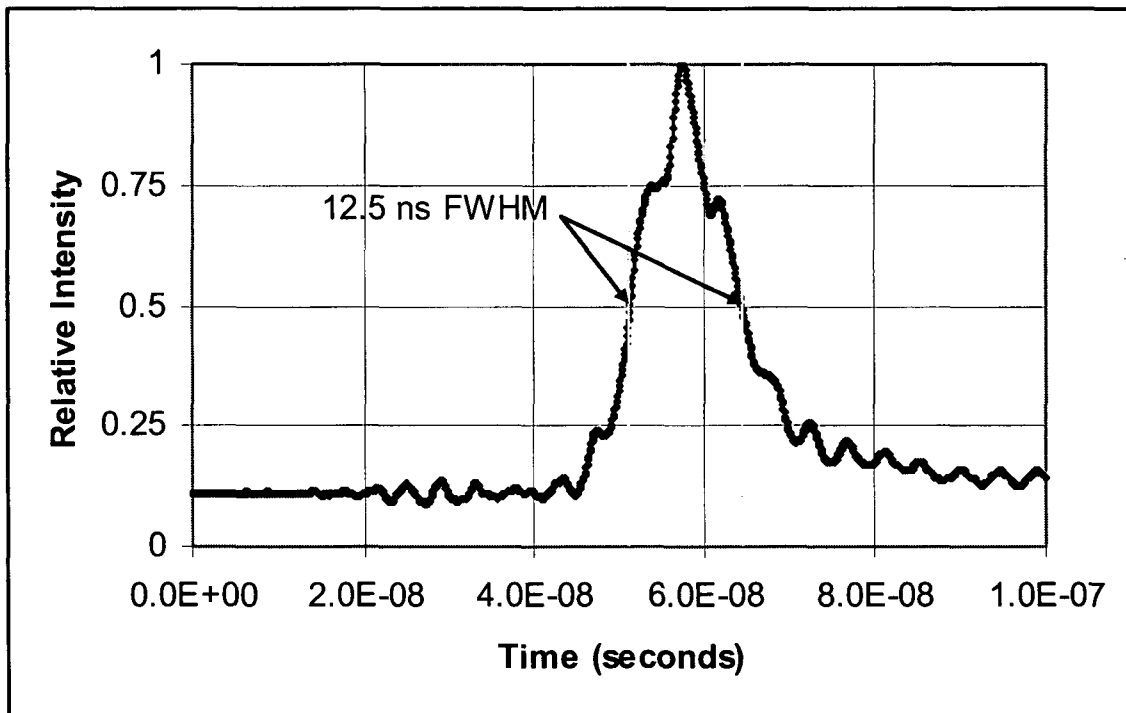


Figure 1. Temporal profile of Nd:YAG laser with average full-width half-maximum (FWHM) of 12.5 ns.

The experimental configuration used in the study is depicted in Figure 2. A 2.5-mm diameter aperture was placed in the incident 6.0-mm diameter laser beam at a distance of one meter from the cornea for beam conditioning. A low-power aiming beam was co-aligned with the test laser and was used to assure co-alignment of the fundus camera with the higher-energy test beam. An 80/20 beam splitter was placed in the coincidental optical path of a fundus camera (Topcon Model TRC 50X) with the higher-power reflected beam being directed through the dilated pupil to the retina of the monkey. The low-power sample of the test laser was directed to an energy meter (Coherent, Model PM-3, S/N 1998A) to document the energy of each retinal exposure. Prior to retinal exposures, a second detector head (Coherent, Model PM-10, S/N 0139F03) was used in the corneal plane to produce a calibration curve (ratio of energy at cornea vs. energy of sample beam) with respect to the sample beam over the planned exposure range.

A visible marker laser (Spectra Physics Model Vanguard) was co-aligned with the test laser and the alignment laser. The exposure duration (100 – 150 ms) of the marker laser was via electronic shutter for optimal marker lesion formation.

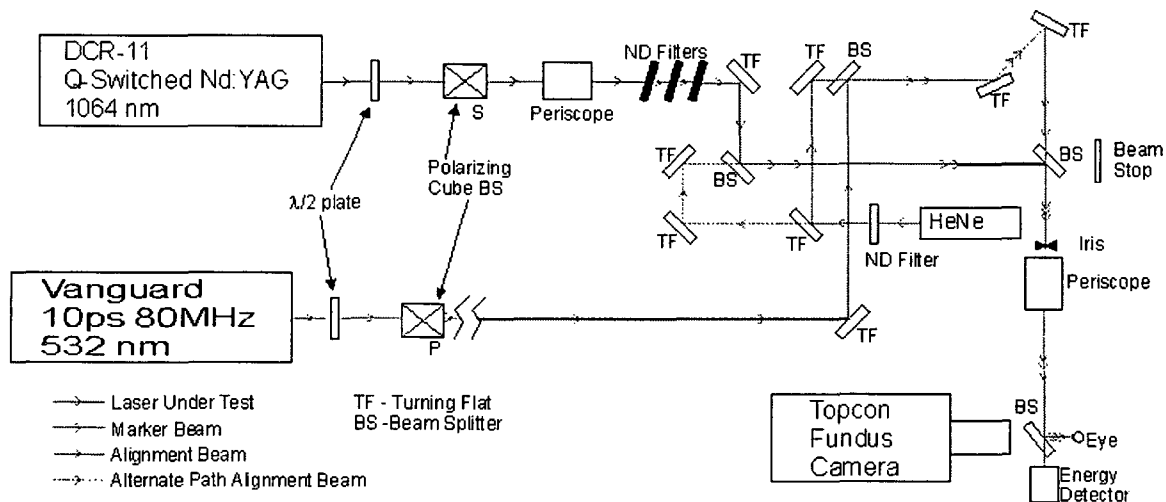


Figure 2. Experimental Configuration

All equipment used in this study was maintained by AFRL/HEDO and was regularly calibrated according to manufacturer specifications. All energy measurement equipment was calibrated to NIST-traceable standards during the period of performance of these experiments.

## 2.2. *In Vivo* Model

Mature Cynomolgus (*Macaca fascicularis*) weighing from 2.2 to 2.9 kilograms were maintained under standard laboratory conditions (12 hours light/ 12 hours dark). All NHPs were screened (pre-exposure) to ensure normal ocular pathology and that no eye was more than one-half diopter from being emmetropic. All procedures were performed during the light cycle of the animal's normal schedule. Animals involved in this study were procured, maintained, and used in accordance with the Federal Animal Welfare Act, the Guide for the Care and Use of Laboratory Animals prepared by the Institute of Laboratory Animal Resources, National Research Council, and the ARVO Resolution for the Use of Animals in Ophthalmic and Vision Research.

## 2.3. *In Vivo* Preparation

Subjects had food withheld for 12 hours prior to the procedure. Each animal was chemically restrained using 10 milligrams per kilogram (mg/kg) ketamine hydrochloride (HCl) intramuscularly. Once restrained, 0.16 mg atropine sulfate was administered subcutaneously. Two drops of proparacaine HCl 0.5%, phenylephrine HCl 2.5%, and tropicamide 1% were each administered to both eyes for cycloplegia and pupillary dilation. Gauze pads were taped over both eyes to protect the eyes and to keep them moistened during transport. Under ketamine restraint, the primate had intravenous catheters (22-24 gauge) placed for administration of an induction dose of propofol (5 mg/kg) and warmed lactated ringers (10 milliliters (ml)/kg/hour flow rate). Propofol anesthesia was maintained with continuous infusion (0.2-0.5 mg/kg/min to effect) via syringe pump. The animal was intubated with a cuffed endotracheal tube. Involuntary extraocular muscular movement was mitigated with a peribulbar injection of 4% lidocaine. In addition to chemical restraint, the animal was physically restrained in the prone position on a specially designed adjustable animal stage for fundus camera observation, laser exposure and fluorescein angiography (FA).

Fluorescein angiography, when performed, was accomplished with intravenous administration of 0.4 ml of 10% Fluorescein (Alcon Laboratories). Approximately 15 minutes prior to Fluorescein administration, acepromazine (0.5-1.0 mg/kg) was administered intravenously as an antiemetic. Core body temperature, oxygen saturation and pulse rate were continuously monitored throughout the study. Body temperature was maintained at normal levels with circulating warm water blankets.

Eyelids of the primates were held open with a wire-lid speculum, and moisture of the cornea was maintained by irrigation with 0.9 percent buffered saline solution. Visualization of the retina during macular laser exposures (25 per

eye) was accomplished with the use of a modified fundus camera. Prior to macular exposures, equally spaced marker lesions (11 per eye) were formed with a frequency-doubled, 532-nm Nd:YAG laser in an L-shaped pattern in the paramacular tissue adjacent to the macula.

Macular exposures delivered with the test laser were localized using marker lesions as fiducial guides. Energy levels for each exposure were randomly selected from a range of energy values expected to bracket the  $ED_{50}$  threshold. The retina of the NHP was observed during laser exposures and photographed post-test with the use of a Topcon fundus camera. Fluorescence angiography was conducted on select animals using the same fundus camera, but with the insertion of a blue barrier filter. During FA, a series of images was acquired at five to 10 second intervals, beginning immediately before insertion of the intravenous dye, and persisting for approximately five minutes.

Three trained examiners evaluated all exposure locations in all eyes, both at one-hour and 24-hours post-exposure. A grade of "yes" or "no" was recorded for each exposure location for each observer. Consensus from two of three observers was required for a final grade of "yes" to be assigned to the retinal response for any exposure. Digitized video and color film photography was used to document the appearance of the retina at the time of the one-hour and 24-hour post-exposure examination. Black-and-white film photography was used to document retinal vascular integrity with FA. After completion of the procedure, the subject was transported back to the prep room where it was monitored for recovery from the anesthetic agents. Upon arousal, the subject was extubated and transported back to the animal housing area.

#### **2.4. Statistical Analysis**

The Probit procedure [16] was used to estimate the  $ED_{50}$  dose for creating a minimal visual lesion (MVL) in the retina. In addition, 95% confidence intervals were calculated from the data. An adequate number of data points were collected to ensure that the magnitude of upper and lower fiducial limits at the  $ED_{50}$  level varied no more than 50%. Furthermore, a Probit-curve slope greater than two, with aggregated-24-hour-observation data, was set as a minimal experimental endpoint.

### 3. RESULTS

Retinal exposures were completed in three eyes of three cynomolgus monkeys. A five-by-five grid pattern of exposures was planned for each eye. In one animal, the exposures were aborted because poor ocular stability allowed delivery of only 20 of the planned 25 exposures.

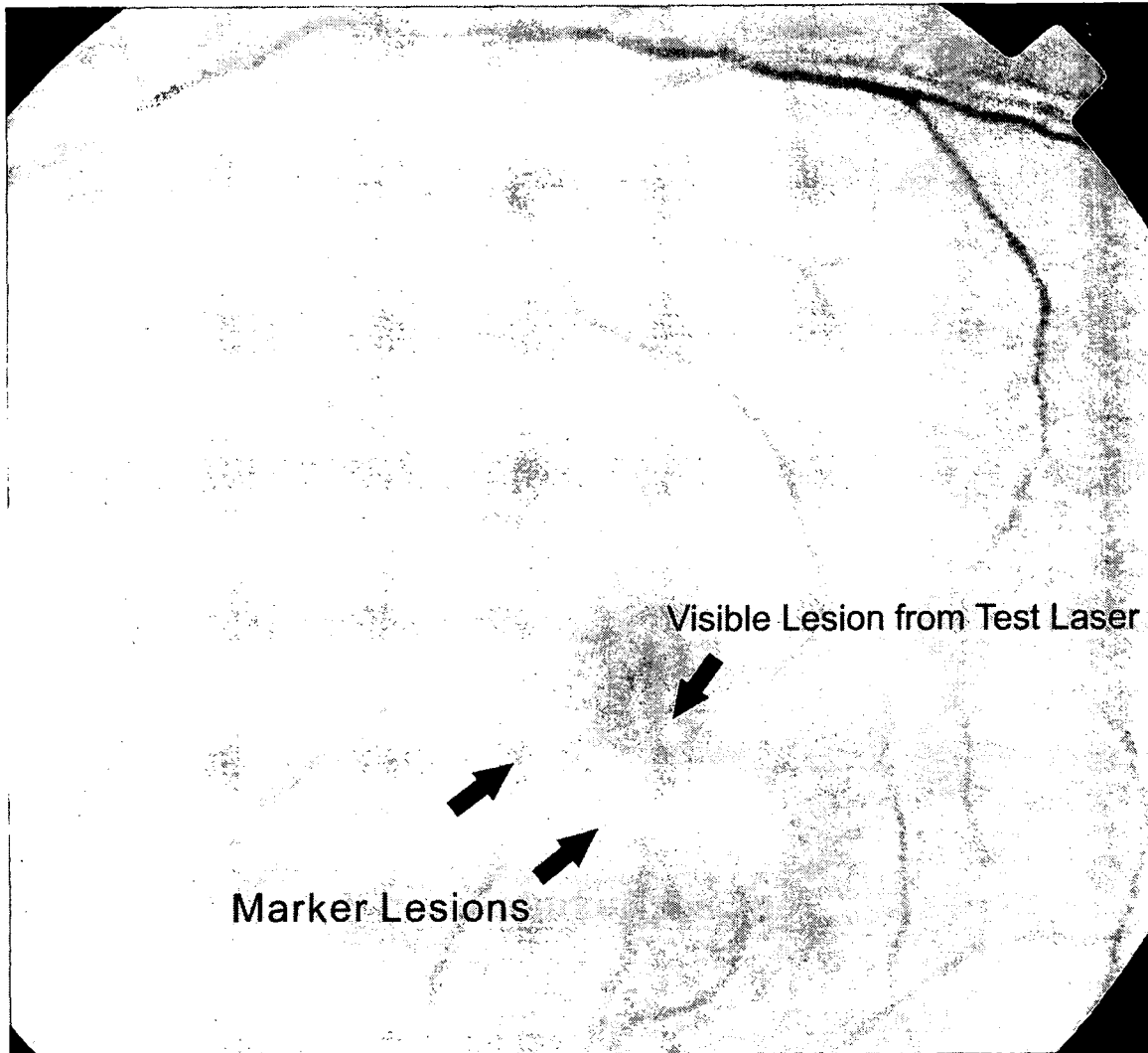


Figure 3. Cynomolgus retinal image from fundus camera indicating marker lesions in an L-pattern and visible lesions apparent at one hour post test with a 12.5-ns laser exposures at 1064 nm.

Fluorescein angiography was completed one-hour post test for one of the three eyes exposed in this study. Figure 4 is one of a series of images captured during the examination. There was no detectable dye leakage in the macula indicating that only sub-hemorrhagic exposure levels were delivered with the test laser.

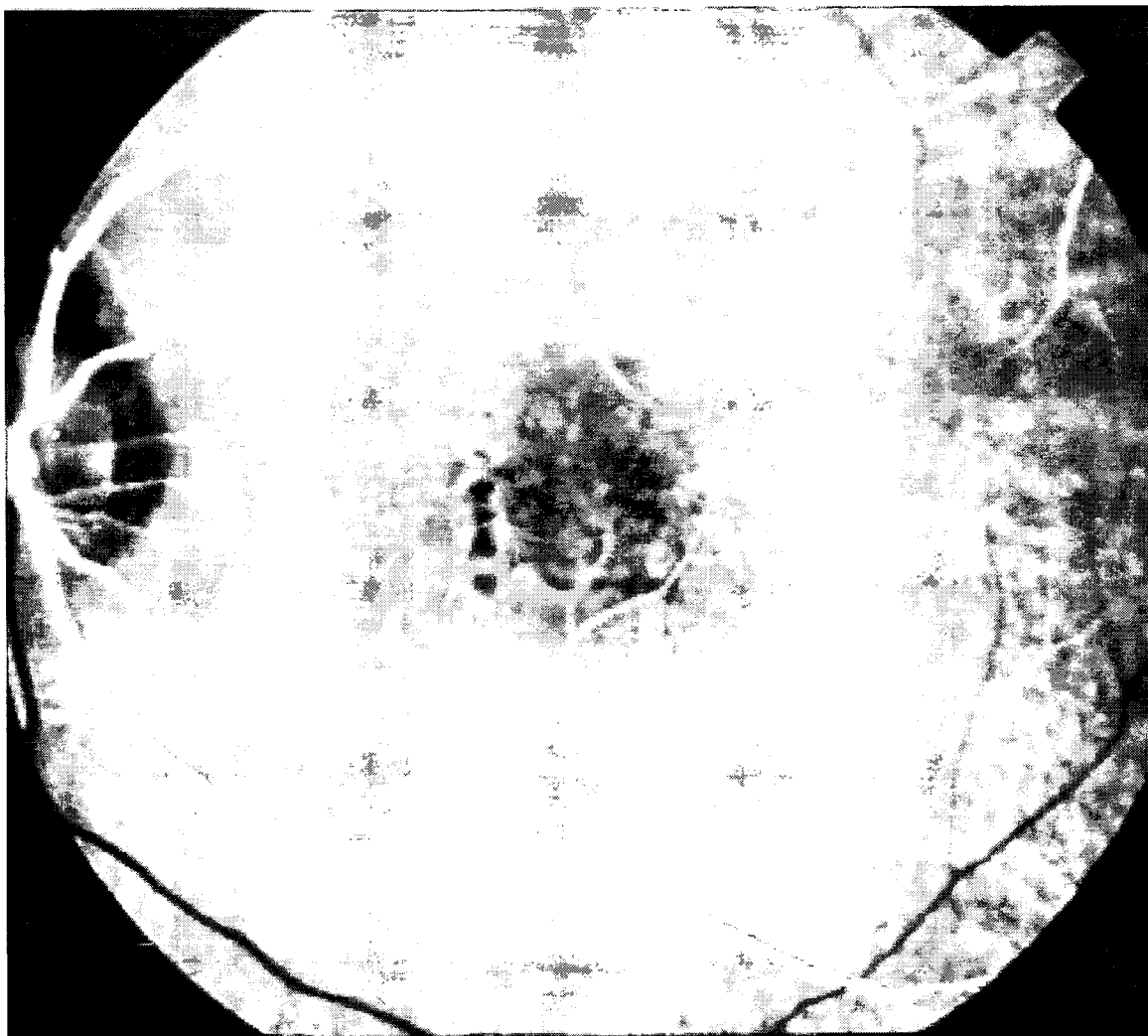


Figure 4. Photograph from fluorescein angiography examination for hemorrhagic lesions.

Probit analysis was performed for retinal dose-response data at one-hour and 24-hours post-exposure. Figure 5 indicates the probability of observing damage at one-hour post-exposure versus the pulse energy delivered at the cornea. Similarly, Figure 6 indicates the probability of observing damage at 24-hours post exposure versus the pulse energy delivered at the cornea.



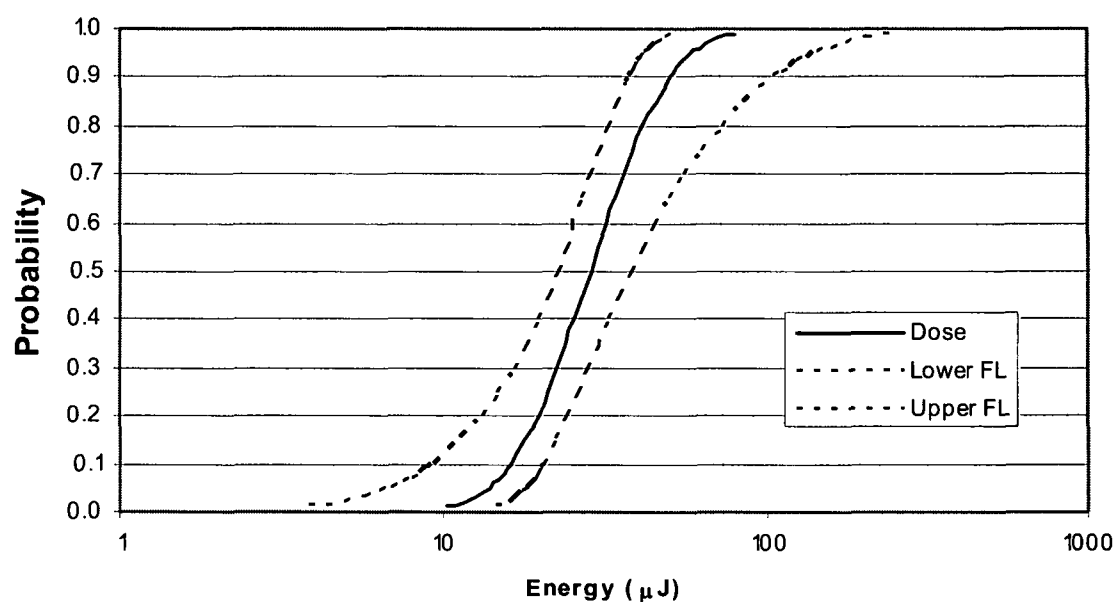


Figure 5. Dose-response data from cynomolgus monkey. Probability of damage one hour post-exposure. ( $\text{ED}_{50} = 28.5 \mu\text{J}$ )

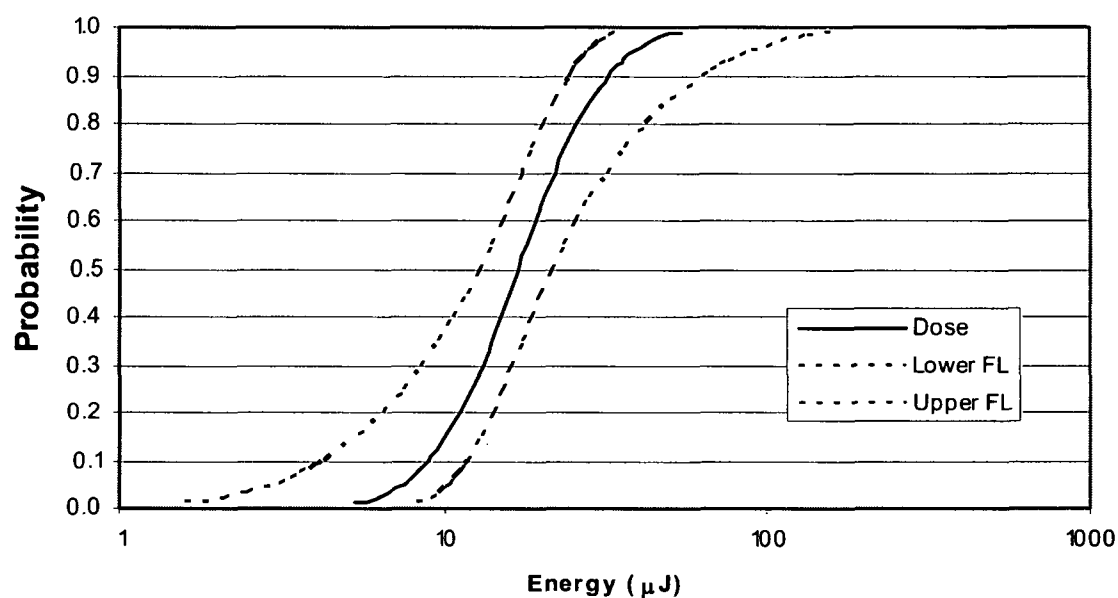


Figure 6. Dose-response data from cynomolgus monkey. Probability of damage 24 hours post-exposure. ( $\text{ED}_{50} = 17.0 \mu\text{J}$ )

The ED<sub>50</sub> Probit data for retinal damage at one- and 24-hours post exposure observation is summarized in Table 3. Slopes for both the one- and 24-hour Probit curves are greater than two, indicating a relatively sharp transition in the retinal response data. The combination of tight fiducial limits and steep slope is an indication of a high quality data set.

Table 3. Summary of ED<sub>50</sub> results for cynomolgus retinal damage with an indication of fiducial limits and slope of Probit curve. (12-ns laser pulse duration,  $\lambda = 1064$  nm)

Observation Time	ED <sub>50</sub>	Lower 95% CI	Upper 95% CI	Slope
1 Hour Data	28.5 $\mu$ J	22.7 $\mu$ J	38.4 $\mu$ J	5.21
24 Hour Data	17.0 $\mu$ J	12.9 $\mu$ J	21.8 $\mu$ J	4.61

#### 4. DISCUSSION

The results of this study utilizing 12-ns exposures in cynomolgus retina compare very favorably to a previously published study conducted by our laboratory using 7-ns exposures with the rhesus retinal damage model [12]. Due to the similarity in experimental configuration and utilization of many of the same personnel from the first study, one would expect the results from the cynomolgus to compare favorably with the rhesus data collected in the prior HEDO study. The Probit results of the one-hour dose-response data from the rhesus study are presented in Figure 7. Correspondingly, Figure 8 contains the dose-response curve for 24-hours post exposure. The ED<sub>50</sub> for damage from the previous HEDO study is summarized in Table 4. As emphasized in Table 5, the results of the current study compare very favorably with the prior study. The ED<sub>50</sub> values for damage for the cynomolgus fall within the fiducial limits as defined by the 95% confidence interval for both the one-hour and 24-hours observation points, suggesting that these values are statistically indistinguishable at the 95 (or higher) percent confidence level [17].

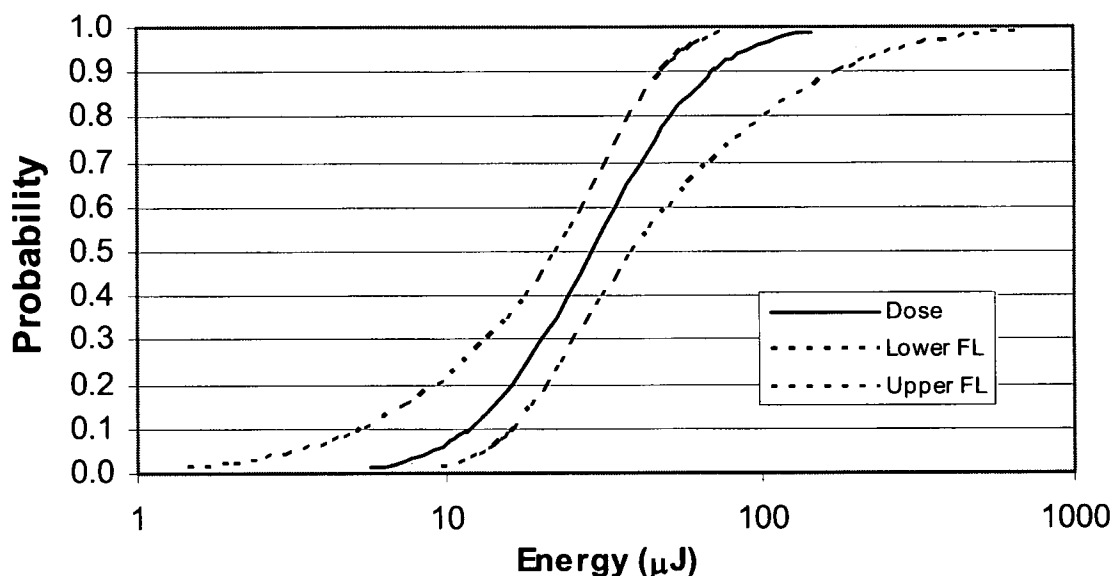


Figure 7. Historical data from retinal exposures in rhesus monkey: probability of damage one hour post exposure (ED<sub>50</sub> = 28.7  $\mu$ J)[12].

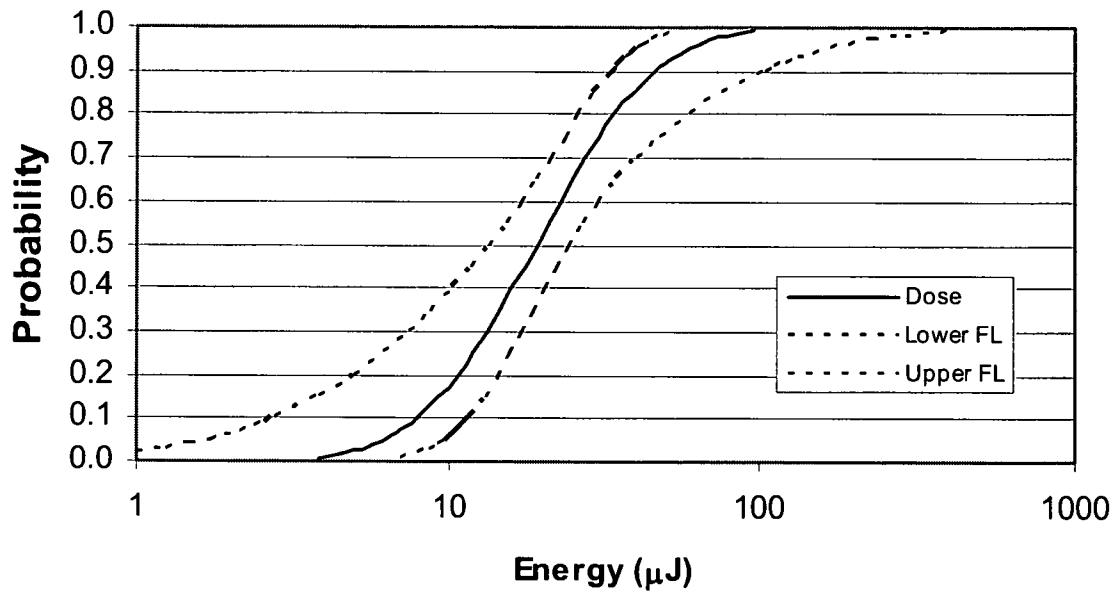


Figure 8. Historical data from retinal exposures in rhesus monkey: probability of damage 24 hours post exposure ( $ED_{50} = 19.1 \mu J$ )[12]

Table 4. Historical  $ED_{50}$  for rhesus retinal damage with 7-ns exposure at 1064 nm [12].

Observation Time	$ED_{50}$	Lower 95% CI	Upper 95% CI	Slope
1-Hour Data	28.7 $\mu J$	22.2 $\mu J$	39.1 $\mu J$	3.29
24-Hour Data	19.1 $\mu J$	13.6 $\mu J$	24.4 $\mu J$	3.35

Table 5. Comparison of  $ED_{50}$  threshold values for damage with rhesus[12] and cynomolgus monkeys.

Animal Model (Duration)	$ED_{50}$ at 1 Hr ( $\mu J$ )	$ED_{50}$ at 24 Hr ( $\mu J$ )
Rhesus (7 ns)	28.7 [22.2-39.1]	19.1 [13.6-24.4]
Cynomolgus (12.5 ns)	28.5 [22.7-38.4]	17.0 [12.9-21.8]

The maximum permissible exposure (MPE) at the cornea at 1064-nm is given in Table 5a of the ANSI standard as,  $MPE = 5.0 \cdot C_C \times 10^{-6} (J \cdot cm^{-2})$ , where  $C_C$  is equal to 1 for the wavelength and geometry in question. This MPE value may be converted from fluence to an energy value by multiplying by the area of the beam assumed by the standard ( $0.385 cm^2$  for a 7 mm pupil). Therefore,  $5 \mu J \cdot cm^{-2} \cdot 0.385 cm^2$  yields an energy limit of 1.92  $\mu J$ . [18]

Table 6 gives a comparison of the ED<sub>50</sub> values obtained for cynomolgus retinal damage with the energy derived from the MPE in the ANSI standard for 1064-nm irradiation.

Table 6. Comparison of ED<sub>50</sub> threshold values to MPE at cornea for retinal protection

Animal Model (Duration)	ED <sub>50</sub> at 1 Hr	ED <sub>50</sub> at 24 Hr	MPE (μJ)
Energy (μJ)	28.5	17.0	1.92
Ratio: ED50/MPE	14.8	8.8	

No vascular leakage was detected using fluorescein angiography. This FA finding was expected over the energy range used in testing for MVL formation (0.26-97.7 μJ) since Allen *et al.* reported the threshold of hemorrhagic lesions at this wavelength and 4-ns pulse duration to be 340 μJ [14]. This hemorrhagic threshold is a factor of three higher than the highest energy exposure delivered in this study.

## 5. CONCLUSION

Cynomolgus monkey (*Macaca fascicularis*) retinas have been irradiated with 12.5-ns pulses of 1064-nm laser irradiation for determination of the suitability of substituting this animal model of retinal laser damage for the established standard, rhesus monkey (*Macaca mulatta*). The ED<sub>50</sub> values obtained for MVL formation in the cynomolgus monkey compare very favorably to rhesus data at both one-hour and 24-hours post-exposure observations. The one-hour ED<sub>50</sub> data value, 28.5 μJ, is less than 1% different than the value obtained with rhesus, 28.7 μJ, while the 24-hour data is approximately 11% less than the rhesus ED<sub>50</sub> data (17.0 μJ vs. 19.1 μJ). Based upon this comparison, the cynomolgus monkey appears to be a suitable replacement for the rhesus for nanosecond laser exposures at 1064 nm, where the damage mechanism is presumed to be photoacoustic in nature.

## ACKNOWLEDGEMENTS

The authors gratefully acknowledge AFOSR Grant Number (2312AH03), and support from the Air Force Research Laboratory Human Effectiveness Directorate. The authors would also like to thank the staff of the Air Force Research Laboratory Veterinary Sciences Branch (AFRL/HEDV) for their expert animal care and handling services. Research Performed by Northrop Grumman was conducted under USAF Contract Number F41624-02-D-7003.

## REFERENCES

1. Madigan, M.C., et al., *Corneal thickness changes following sleep and overnight contact lens wear in the primate (Macaca fascicularis)*. Curr Eye Res, 1987. **6**(6): p. 809-15.
2. Kaufman, P.L., B.T. Calkins, and K.A. Erickson, *Ocular biometry of the cynomolgus monkey*. Curr Eye Res, 1981. **1**(5): p. 307-9.
3. Crawford, K.S., P.L. Kaufman, and L.Z. Bito, *The role of the iris in accommodation of rhesus monkeys*. Invest Ophthalmol Vis Sci, 1990. **31**(10): p. 2185-90.
4. Ollivier, F.J., et al., *Corneal thickness and endothelial cell density measured by non-contact specular microscopy and pachymetry in Rhesus macaques (Macaca mulatta) with laser-induced ocular hypertension*. Exp Eye Res, 2003. **76**(6): p. 671-7.
5. Drexler, W., et al., *Biometric investigation of changes in the anterior eye segment during accommodation*. Vision Res, 1997. **37**(19): p. 2789-800.
6. Koretz, J.F., A. Rogot, and P.L. Kaufman, *Physiological strategies for emmetropia*. Trans Am Ophthalmol Soc, 1995. **93**: p. 105-18; discussion 118-22.

7. Eysteinnsson, T., et al., *Central corneal thickness, radius of the corneal curvature and intraocular pressure in normal subjects using non-contact techniques: Reykjavik Eye Study*. Acta Ophthalmologica Scandinavica, 2002. **80**(1): p. 11-15.
8. Meyer-Riemann, W., J. Petersen, and M. Vogel, *[Accidental macular injuries caused by the neodymium:YAG laser]*. Klin Monatsbl Augenheilkd, 1997. **211**(2): p. 122-7.
9. Toth, C.A., et al., *Retinal effects of ultrashort laser pulses in the rabbit eye*. Invest Ophthalmol Vis Sci, 1995. **36**(9): p. 1910-7.
10. Goldman, A.I., W.T. Ham, Jr., and A.H. Mueller, *Ocular damage thresholds and mechanisms for ultrashort pulses of both visible and infrared laser radiation in the rhesus monkey*. Exp Eye Res, 1977. **24**(1): p. 45-56.
11. Goldman, A.I., W.T. Ham, Jr., and H.A. Mueller, *Mechanisms of retinal damage resulting from the exposure of rhesus monkeys to ultrashort laser pulses*. Exp Eye Res, 1975. **21**(5): p. 457-69.
12. Cain, C.P., et al., *NEAR-INFRARED ULTRASHORT PULSE LASER BIOEFFECTS STUDIES*. 2003, AFRL/HEDO: Brooks City-Base, TX.
13. Ham, W.T., Jr., et al., *Ocular hazard from picosecond pulses of Nd: YAG laser radiation*. Science, 1974. **185**(148): p. 362-3.
14. Allen, R.G., et al., *Ocular effects of pulsed Nd laser radiation: variation of threshold with pulsewidth*. Health Phys, 1985. **49**(5): p. 685-92.
15. Lund, D.J. and E.S. Beatrice, *Near infrared laser ocular bioeffects*. Health Phys, 1989. **56**(5): p. 631-6.
16. Finney, D.J., *Probit analysis*. 3rd ed. 1971, Cambridge: Cambridge University Press.
17. Payton, M.E., M.H. Greenstone, and N. Schenker, *Overlapping confidence intervals or standard error intervals: What do they mean in terms of statistical significance?* Journal of Insect Science, 2003: p. 1-6.
18. (ANSI), A.N.S.I., *Maximum permissible exposure (MPE) for small-source ocular exposure to a laser beam*. 2000, American National Standard.